Title: Brain connectome mapping of complex human traits and their polygenic architecture using machine learning

Short title: Connectome mapping of human traits and genetics

Luigi A. Maglanoc[1,2], Tobias Kaufmann[2], Dennis van der Meer[2,3], Andre F. Marquand[4,5], Thomas Wolfers[1,2], Rune Jonassen[6], Eva Hilland[1,7], Ole A. Andreassen[2], Nils Inge Landrø[1], Lars T. Westlye[1,2]

[1] Department of Psychology, University of Oslo, Oslo, Norway
[2] NORMENT, Institute of Clinical Medicine, University of Oslo & Division of Mental Health and Addiction, Oslo University Hospital, Oslo, Norway
[3] School of Mental Health and Neuroscience, Faculty of Health, Medicine and Life Sciences, Maastricht University, The Netherlands
[4] Donders Centre for Cognitive Neuroimaging, Donders Institute for Brain, Cognition and Behaviour, Radboud University, Nijmegen, The Netherlands
[5] Department of Neuroimaging, Institute of Psychiatry, King's College London, London, UK
[6] Faculty of Health Sciences, Oslo Metropolitan University, Oslo, Norway
[7] Division of Psychiatry, Diakonhjemmet Hospital, Oslo, Norway

Corresponding authors: Luigi A. Maglanoc (luigi_maglanoc@hotmail.com) & Lars Westlye (l.t.westlye@psykologi.uio.no), Department of Psychology, University of Oslo, Pb. 1094, Blindern, 0317 OSLO, Norway

Keywords: fMRI, functional connectivity, human traits, polygenic scores, machine learning

Number of words in abstract: 248

Number of words in article body: 3974

Number of figures: 5

Number of tables: 1

Number of supplemental information: 1 (2 tables and 31 figures)

Abstract

Background: Mental disorders and individual characteristics such as intelligence and personality are complex traits sharing a largely unknown neuronal basis. Their genetic architectures are highly polygenic and overlapping, which is supported by heterogeneous phenotypic expression and substantial clinical overlap. Brain network analysis provides a non-invasive means of dissecting biological heterogeneity yet its sensitivity, specificity and validity in assessing individual characteristics relevant for brain function and mental health and their genetic underpinnings in clinical applications remains a challenge.

Methods: In a machine learning approach, we predicted individual scores for educational attainment, fluid intelligence and dimensional measures of depression, anxiety and neuroticism using fMRI-based static and dynamic temporal synchronization between large-scale brain network nodes in 10,343 healthy individuals from the UK Biobank. In addition to age and sex to serve as our reference point, we also predicted individual polygenic scores for related phenotypes, and 13 different neuroticism traits and schizophrenia.

Results: Beyond high accuracy for age and sex, supporting the biological sensitivity of the connectome-based features, permutation tests revealed above chance-level prediction accuracy for trait-level educational attainment and fluid intelligence. Educational attainment and fluid intelligence were mainly negatively associated with static brain connectivity in frontal and default mode networks, whereas age showed positive correlations with a more widespread pattern. In contrast, prediction accuracy was at chance level for depression, anxiety, neuroticism and polygenic scores across traits.

Conclusion: These novel findings provide a benchmark for future studies linking the genetic architecture of individual and mental health traits with fMRI-based brain connectomics.

Introduction

Mental disorders such as depression, anxiety and schizophrenia have joint high prevalence, early onset, and often a persistent nature (1). Therefore, identifying neuroimaging-based biomarkers which may facilitate early risk detection and stratification and monitoring of interventions of mental disorders is a global aim for the clinical neurosciences potentially implicating millions worldwide (2–4). Twin and family studies have documented a strong genetic contribution across a range of human traits including mental disorders (5), and high polygenicity based on genome-wide associations studies (GWAS)(6–10). Neuroticism is a personality trait which exacerbates vulnerability towards mental disorders (11), supported by both genetic correlations (12–14) and pleiotropy (15) with mental health traits. Educational attainment and fluid intelligence are two related and heritable phenotypes associated with a range of behaviors and outcomes (16) such as occupational attainment and social mobility (17), brain measures (18–20), mental health (21, 22) and more general aspects of health (23, 24). Further, they show strong genetic correlations across cognitive domains and levels of ability (25).

Both the structural and functional architecture of the brain are heritable traits (26), and studies reporting aberrations in fMRI measures of brain connectivity in mental disorders are abundant (27–29). However, the generalizability, robustness and clinical value of the findings have been questioned (30–32). This lack of consistency and generalizability is likely partly due to differences in power (33, 34), sample characteristics and analytical methods (35), but also the vast clinical heterogeneity of mental disorders (36–38). Further, although a substantial heritability of brain measures has been demonstrated (26, 39, 40), the sensitivity of fMRI features to the cumulative genetic risk, e.g. as reflected in polygenic risk scores (the sum of risk variants weighted by their effect size in a GWAS), for brain and mental health related traits is debated.

Studies assessing the heritability and clinical associations with fMRI resting-state brain functional connectivity (FC) have typically targeted estimates of static FC (sFC), defined as the average temporal correlation between two brain regions. Less is known about the associations with dynamic properties of FC (dFC), conceptualized as the fluctuation in temporal correlations between two brain regions. Further, fMRI-based FC reflects the joint contribution of partly independent sources oscillating at specific frequency bands (41), which are tied to a range of neural processes (42) and cognitive functions (43). Mapping the brain functional connectome to the genetic architecture of mental health traits may inform nosological and mechanistic studies and, in the long run, improve diagnostics, prevention and treatment of mental disorders.

Here, we tested the predictive value of static and dynamic measures of brain connectivity for (i) traits relevant for individual adaptation (e.g. educational attainment) and brain and mental health, and age and sex, and (ii) polygenic scores of related traits. We used resting-state fMRI data from 10,343 healthy individuals from the UK Biobank (UKB) in a machine learning approach. Individual traits included years of educational attainment, fluid intelligence, and dimensional measures of depression, anxiety and neuroticism. We also calculated and predicted the individual polygenic scores for educational attainment, fluid intelligence, depression, schizophrenia, anxiety, and 13 neuroticism traits, based on previous genome-wise association studies (GWAS). We employed cross-validation and evaluation of model performance to reduce bias and overfitting, in addition to permutation testing for statistical inference. We expected moderate and relatively low yet above chance-level predictive value for the phenotypes and the polygenic scores respectively. Further, we anticipated overall similar rankings of the brain connectivity features for the traits and their respective polygenic scores. Lastly, based on a general positive-negative mode of covariation

between fMRI-based connectivity and complex human traits (44), we anticipated that similar brain networks would be relevant for predicting the various traits.

Materials and Methods

Sample

We used the October 2018 release of UKB imaging data (45), comprising 12,213 individuals with resting-state fMRI scans that passed the quality control performed by the UKB (46, 47), including assessment of head motion (47). The exclusion criteria across all were individuals with an ICD-10 based mental or a neurological disorder (N = 210) to represent the general population, and non-white Europeans (N = 1659) yielding a total of 10,343 individuals. All participants provided informed consent prior to enrolment, and the study has been approved by the South-Eastern Norway Regional Committees for Medical and Health Research Ethics (REC).

Phenotype data

Neuroticism was calculated based on a previous implementation (13), while years of educational attainment was based on the "qualifications" variable (UKB field: 6138) following a recent imputation procedure (48). Fluid intelligence (UKB field: 20016) was defined as the sum of the number of correct answers on the verbal-numerical reasoning test (13 items). Data for all the aforementioned phenotypes were taken from instance 2 (imaging visit). Symptom load for depression and anxiety were based on the sum score from the 9-item Patient Health Questionnaire (PHQ-9) and the 7-item Generalized Anxiety Disorder (GAD-7) questionnaire, respectively, were taken from the online follow-up. Table S1 shows the number of individuals included for each phenotype and all polygenic scores. Figure 1 shows a correlation plot of all the phenotypes.

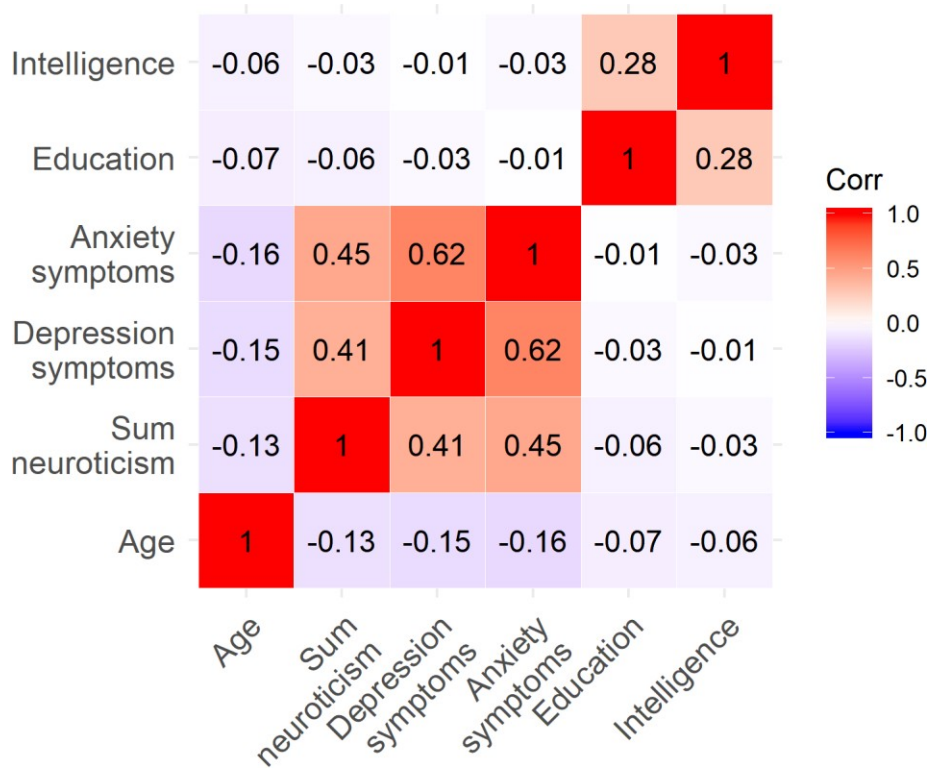

Figure 1. Heatmap of the correlation (Spearman's rho) between the phenotypes. Sex is notshown because it is a categorical variable.

Polygenic scores

Procedures for DNA collection and genotyping in UKB have been described previously (49). Polygenic scores were calculated using PRSice v.1.25 (50) based on GWAS results for broad depression, probable major depressive disorder (MDD; 49), diagnostic MDD (9), item-level and sum neuroticism (13), anxiety (52), and schizophrenia (8). For polygenic scores based on item-level and sum neuroticism, educational attainment and fluid intelligence (6, 7) we performed our own GWAS (see Supplemental Methods and Materials) to avoid overlap in participants in the discovery and target dataset (i.e. fMRI sample). For the main polygenic

score analyses, the single nucleotide polymorphism (SNP) inclusion threshold was set at $p \leq$

0.5, as this typically explains more variance in the clinical phenotype (53). Supplemental Figure S1 shows the distribution of each polygenic score, and Supplemental Figure S2 shows a correlation plot with a dendrogram based on hierarchical clustering across all polygenic scores. For sensitivity analyses, we repeated the analyses using a threshold of $p \leq 0.05$, and also derived a polygenic score based on the first component from a principal component analysis (PCA) performed on the polygenic scores from thresholds $p \leq 0.001$ to $p \leq 0.5$ (at 0.001 intervals), as in a recent implementation (54) (see Supplemental Figures 12 to 31).

Image Acquisition and pre-processing

Detailed description of the image acquisition, pre-processing, group-level ICA and dual regression can be found elsewhere (46) and was carried out by the UK Biobank (47). The majority of the MRI data used were obtained in Cheadle Manchester on a Siemens Skyra 3T scanner (Siemens Medical Solutions, Germany) with a 32-channel head coil. A small number of scans (N = 354) were obtained at an identical scanner in Newcastle. FSL (http://fsl.fmrib.ox.ac.uk/fsl) was used for fMRI data preprocessing. Briefly this involved motion correction, high-pass temporal filtering, echo-planar image unwarping, gradient distortion correction unwarping, and removal of structured artifacts. Estimated mean relative in-scanner head motion (volume-to-volume displacement) was computed with MCFLIRT. Group-level ICA was carried using MELODIC based on 4,162 datasets. The model order of 25 was chosen to yield common large-scale functional networks such as the default mode network (DMN), and because estimation of nodes and corresponding edges tend to be more robust at lower than higher model orders. Four of these ICs were identified as noise and discarded, leaving a total of 21 ICs for analyses. Dual regression was performed to generate subject specific spatial maps and corresponding time-series.

Functional connectivity measures

All FC measures were computed in MATLAB. SFC was computed both with the unfiltered and bandpass filtered time-series within 0.04-0.07 Hz. For both, a node-by-node connectivity matrix was created using partial correlations between the subsequent time-series (55), resulting in 210 unique edges. These partial correlations were L1-regularized, with estimated regularization strength (lambda) at the subject level (56–58).

For dFC we used a phase-based method (59) within the 0.04-0.07 Hz frequency band (60). Briefly, this method is sensitive to the degree of coupling and de-coupling between pairs of brain networks across the scanning session, based on applying the Hilbert transform and subsequently the Kuramoto order on the node time-series. This resulted in 210 unique edges, representing the oscillation between each of the 21 ICs at every instant (61).

Statistical analysis

All statistical analyses were performed in R version 3.4.2 (62). We z-normalized all polygenic scores prior to the machine learning analyses.

Machine learning analyses

In our primary analyses, we tested to what extent various combinations of static and dynamic FC ("feature sets")between all nodes in an extended brain network could predict the phenotypes, by using shrinkage linear regression (63) implemented in the R-package 'care' (http://strimmerlab.org/software/care). Briefly, a linear model is fit which calculates regression coefficients based on shrinkage estimates of correlations and variances. Firstly, 80% of the data was used as the training set while the remaining 20% of the data was used as the left-out test set. We ran 10-fold internal cross-validation on the training set (i.e. based on iteratively using 90% of the sample to predict the remaining 10%), repeated 100 times on

randomly partitioned data. We computed root mean square error (RMSE) as our main measure of model performance for all phenotypes, but also mean absolute error (MAE) and R^2 (explained variance or model fit). R^2 was mainly used to visualize and compare model performance across models. We also used Spearman's *rho* (or Pearsons's r for age) as a measure for model performance for predicting these phenotypes. For sex, we used logistic regression for classification and report accuracy, sensitivity, specificity and cohen's kappa as measures of model performance. The same model parameters were used in the model validation, by using the whole training set to predict the phenotypes in the left-out test set. Statistical significance for phenotypes were assessed for the best feature set with a positive R^2 by generating null-distributions using permutation-based testing. The mean model performance from cross-validation of the empirical data was used as our point estimate. The null distributions were generated by running identical cross-validated prediction models on randomly shuffled target variables (i.e. phenotype scores) across 10,000 iterations. Then, the corrected p-value was computed by comparing the RMSE from cross-validation of the true data to the 10,000 RMSE estimates from cross-validation of the permuted datasets. We ran unpaired t-tests to statistically compare the prediction accuracy of certain feature sets for specific phenotypes based on each of the 100 estimates from cross-validation. For the phenotype models that were statistically significant, we determined the relative importance of each edge by computing the mean correlation-adjusted marginal correlation (CAR) scores (64) in cross-validation. Briefly, CAR-scores are the correlation between the phenotypes (or polygenic scores) and the Mahalanobis-decorrelated edges (i.e. after reducing autocorrelation amongst the edges by a linear transform) (65). We also assessed the correlation amongst these models based on the CAR-scores. To assess the confounding effects of age, sex and head motion, we repeated the analyses for fluid intelligence by regressing these confounders from the edges in the sFC feature set. We used the same framework to predict polygenic

scores, computing Pearson's r instead of Spearman's rho, and model validation for the main PGRS analyses ($p \leq 0.5$). To assess the effect of population stratification (i.e. systematic genetic differences due to ancestry), we regressed out the first 10 genetic principal components (UKB field: 22009) from the edges of the best feature set for one of the polygenic score models. We also assessed the correlation amongst phenotypes and corresponding polygenic scores based on the CAR-scores in the cases where the phenotype model was statistically significant.

Results

Machine learning prediction of phenotypes

Figure 2 shows the distribution of the phenotypes and cross-validated results of the overall best feature set (sFC). Permutation testing revealed moderate yet above chance-level prediction accuracy for phenotypic level educational attainment, fluid intelligence, and high prediction accuracy for age (Table 1), and sex (mean accuracy = 0.781, accuracy SD = 0.0139, corrected $p < 0.0027$, sensitivity = 0.754, specificity = 0.806, cohen's kappa = 0.560). In comparison, predictions of dimensional measures of depression, anxiety and neuroticism anxiety performed at chance level (Table 1). Supplemental Figures S3 provides the cross-validated results of the other FC feature sets (see Supplemental Figure S4 for the sex results). The feature set with all three FC-types (sFC, bandpass filtered sFC, and dFC) resulted in marginally higher prediction accuracy than the sFC feature set only for age ($t = 85.613$, df = 170.83, $p < 0.001$) and sex ($t = 64.961$, df = 171.67, $p < 0.001$). The model validation results were very similar to the cross-validated results (Supplemental Figure S5). Sensitivity analyses predicting age using the sFC feature set showed that there was very little difference when regressing scanner site out of the edges or excluding participants scanned in Newcastle (n=354, Supplemental Figure S6A). Further sensitivity analyses predicting fluid intelligence

using the sFC feature set showed similar results when regressing out age (linear and quadratic), sex and head motion from the edges (see Supplemental Figure S6B).

Supplemental Figure S7 shows the grouping of brain networks based on hierarchical clustering (Supplemental Methods and Materials) and Figure 3 shows the top 20 edges in the sFC feature set for trait-level educational attainment and fluid intelligence based on feature importance (CAR scores). Briefly, we observed mainly negative associations with sFC for educational attainment, particularly within DMN and frontal network nodes, and a similar pattern for fluid intelligence. In contrast, the CAR scores revealed largely positive associations between sFC and age, mainly within the cluster of motor/somatosensory and attentional networks, and within the cluster of default mode and frontal networks. Figure 4 shows the top 40 edges that were positively associated with each phenotype, based on the feature set using all three FC-types, suggesting that these are largely non-overlapping. In short, based on feature importance, we observed roughly equal amounts of edges across all three FC-types for educational attainment (sFC = 16 edges, bandpass filtered sFC = 12 edges, dFC = 12 edges). We observed only two edges based on bandpass filtered sFC between visual networks and the cluster of default mode and frontal networks for fluid intelligence and only three edges based on dFC for age. Table S2 shows the correlation between the FC-types for age, fluid intelligence and educational attainment. See Supplemental Results for the correlations between phenotypes based on specific specific feature sets.

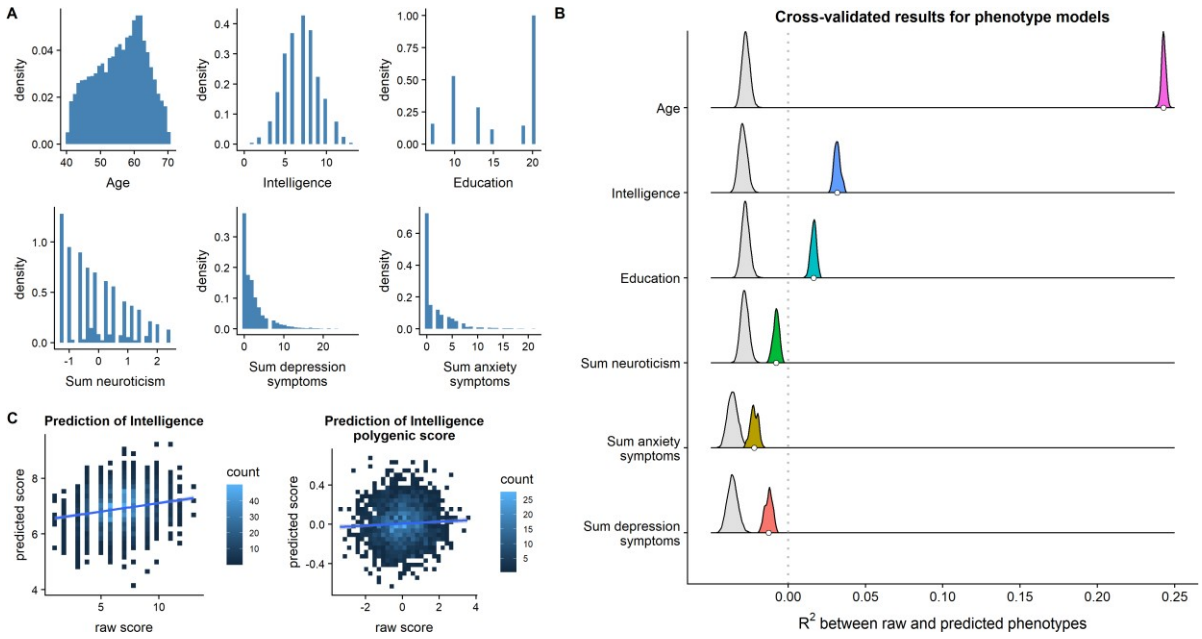

Figure 2. (A) The distribution of all the phenotypes we used in the machine learning analyses (see Supplemental Figure S4 for sex results). (B) The coloured density distributions represent the cross-validated results (across 100 repetitions) of the best FC feature set (sFC: the mean is denoted by the white circles) for a given phenotype, using R^2 as our metric of model performance. The grey distributions represent the mean model performance for each of the 10,000 permuted datasets. Although RMSE is our main metric of model performance, R^2 allows for comparison across phenotypes and polygenic risk scores. R^2 is negative for some of the models because we are testing it out-of-sample, meaning that the model can be arbitrarily bad. (C) Associations between raw and predicted scores for phenotypic level intelligence (left) and polygenic score (right). Education pertains to the years of educational attainment

	RMSE (mean, SD)	*p*-value	Correlation	MAE	R^2
Phenotypes					
Educational attainment	4.739 (0.0643)	< 0.0027	0.1634	4.348	0.0164
Fluid intelligence	2.043 (0.0505)	< 0.0027	0.2014	1.638	0.0317
Age	6.482 (0.1296)	< 0.0027	0.4947	5.317	0.2428
Neuroticism	0.984 (0.0206)	1	0.0924	0.8201	-0.0078
Depression	3.383 (0.2126)	1	0.0947	2.353	-0.0126
Anxiety	3.222 (0.1978)	1	0.0616	2.270	-0.0220
Polygenic scores					
Educational attainment	0.997 (0.0249)	1	0.0941	0.7926	-0.0061
Fluid intelligence	1.002 (0.0240)	1	0.0553	0.8009	-0.0163
Worry	1.007 (0.0226)	1	0.0670	0.8170	-0.0138

Table 1: Mean model performance measures from cross-validation for all the phenotypes and polygenic scores with high correlation-based model performance using the sFC feature set. Worry is one of the 13 neuroticism traits. Correlation was based on Spearman's rho for the phenotypes and Pearson's r for the polygenic scores. The *p*-value is calculated using permutation testing (based on RMSE), with an additional Bonferroni correction.

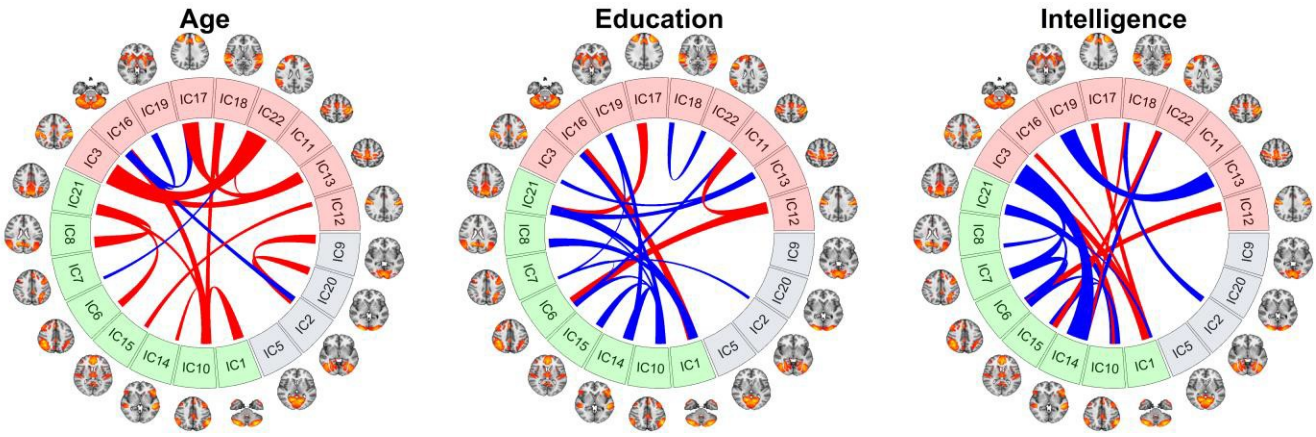

Figure 3. The top 20 edges based on CAR-scores for the best FC feature set (sFC) for age, years of education and fluid intelligence. The thickness of the lines represents the relative importance of each edge for that specific feature set. Red and blue lines indicate that the feature is positively and negatively associated with the phenotype respectively, when considering all the features. The brain networks are grouped into 3 clusters based on hierarchical clustering (see the Supplemental Methods and Supplemental Figure S8) which roughly represent the motor/somatosensory and attentional networks (red), default mode and frontal networks (green), visual components (blue).

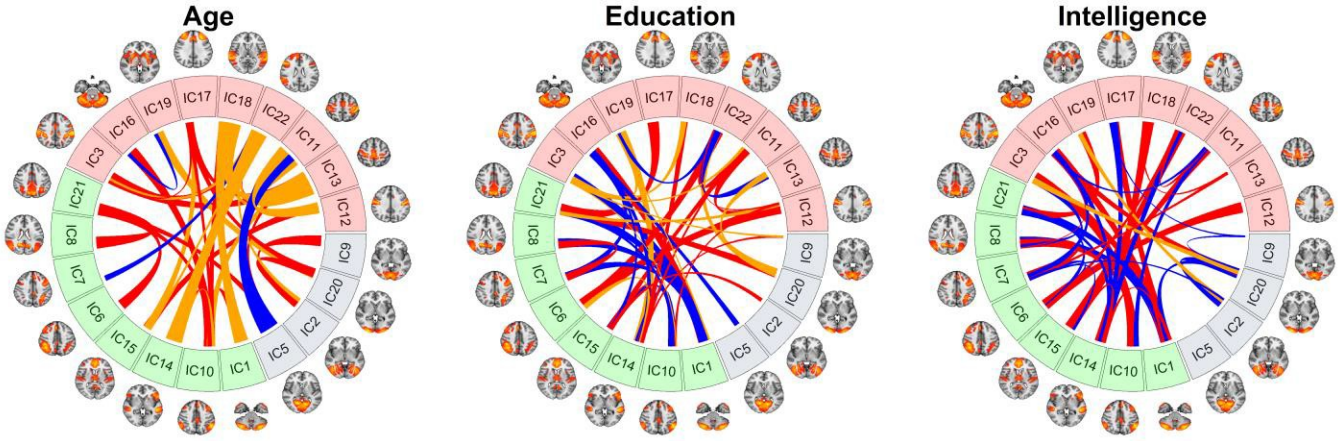

Figure 4. The top 40 edges based on CAR-scores from cross-validation for the feature set that includes sFC (red), bandpass filtered sFC (orange) and dFC (blue). These represent the relative importance of each edge associated with the specific trait, with the thickness of the line signifying the relative order.

Machine learning prediction of polygenic scores

Model performance for all polygenic scores (depression, anxiety, schizophrenia, neuroticism traits, educational attainment and intelligence) were low and had negative explained variance (based on R^2) across feature sets (Supplemental Figure S8). We only performed permutation testing for the polygenic scores that showed higher correlation-based model performance, including educational attainment, fluid intelligence and worry (Table 1). Figure 5 provides an

illustrative example of moderate model performance (phenotypic level educational attainment) and low model performance (educational attainment polygenic scores) showing cross-validated results on empirical and permuted data. The model validation results are very similar to the cross-validated results (Supplemental Figure S9). There was little difference when controlling for population stratification in the sFC feature set predicting educational attainment polygenic risk scores (Supplemental Figure S6C). Cross-validated results were similar using a lower polygenic score threshold ($p \leq 0.05$: Supplemental Figure S10), and the first component from PCA across thresholds (Supplemental Figure S11). See Supplemental Results for the correlations between phenotypes and their corresponding polygenic scores based on specific specific feature sets.

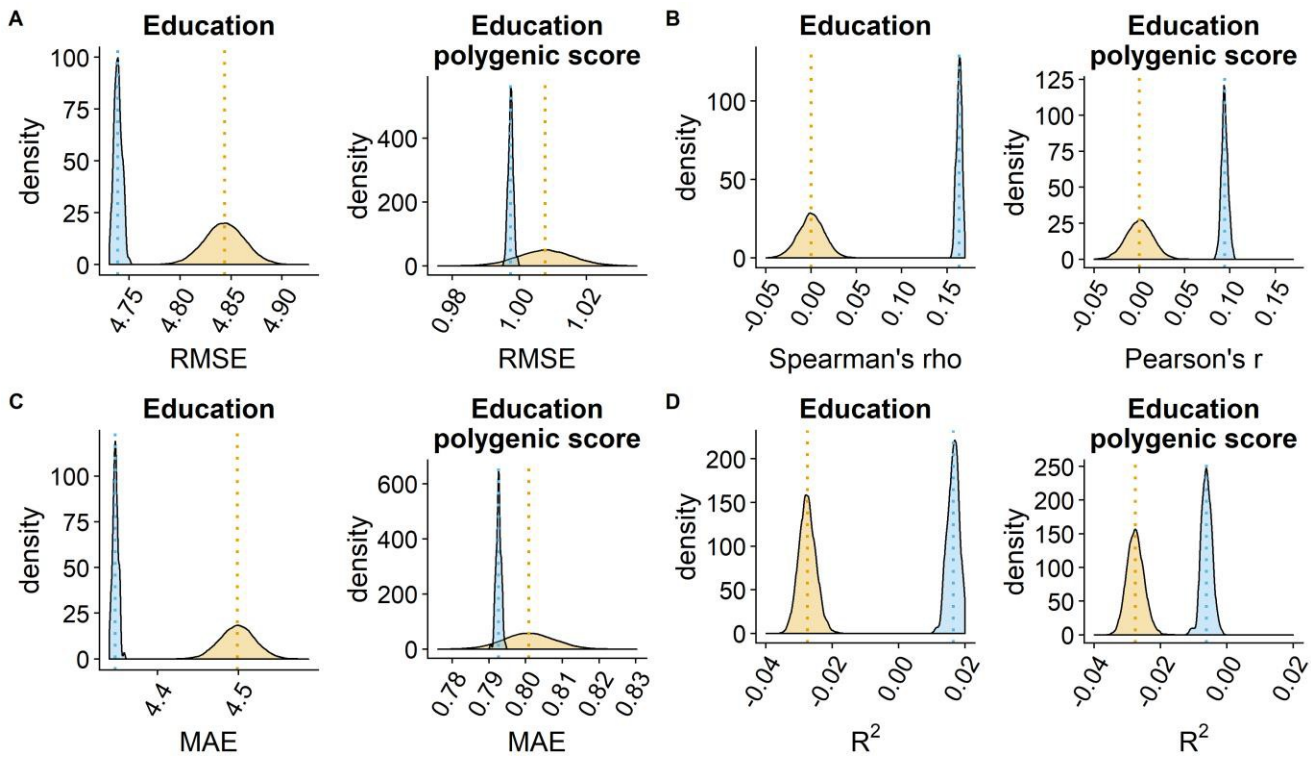

Figure 5. Cross-validated results comparing phenotypic level years of educational attainment and polygenic scores. For each plot, the blue represents model performance for each repetition (100) of the empirical data, and orange represents the mean model performance for each of the 10,000 permuted datasets (orange) based on (A) RMSE, (B) Correlation, (C) mean absolute error (MAE), and (D) R^2. The lines denote the mean of the respective distributions.

Discussion

Recent advances have led to an increasing interest in mapping the brain connectomic landscape underlying (i) traits relevant for brain and mental health and (ii) their genetic underpinnings. To this end, we conducted a large-scale integration of advanced measures of fMRI-based brain functional connectivity in a population cohort of 10,343 healthy individuals. First, we show that individual differences in educational attainment and fluid intelligence, which have high relevance for life satisfaction and real-world outcomes, are partly reflected in the temporal organization of the brain. Furthermore, we demonstrate high prediction accuracy for age and sex, which supports the sensitivity of the approach. In contrast to our expectations, we found chance-level performance for individual level prediction of dimensional measures of depression, anxiety and neuroticism, and also for polygenic scores for depression, anxiety, schizophrenia, neuroticism traits, educational attainment and intelligence.

We obtained moderate yet above chance-level prediction accuracy for educational attainment and corresponding high feature importance for the DMN and frontal networks. We also obtained moderate yet significant prediction accuracy for fluid intelligence, in line with the literature (66–69). This was largely driven by negative correlations between intelligence and sFC amongst frontal and DMN networks, suggesting relative dedifferentiation (i.e. increased negative FC) between the DMN and frontal regions in individuals with higher intelligence. This pattern was largely overlapping with the results for educational attainment, consistent with a study using a subset of the current sample (19), and also reflected in a strong positive correlations between the feature importance from the two prediction tasks.

Highest model performance across all traits was observed for age, in line with several studies showing high age-sensitivity of functional imaging features (70–73). In general, compared to educational attainment and intelligence, we observed a more distributed pattern

of the edge-wise feature importance for the age prediction. This suggests that individual differences in educational attainment and intelligence may be more confined to specific parts of the brain connectome than the effects of aging, which are more pervasive.

To date, there is a lack of functional imaging studies comparing the sensitivity and predictive accuracy of dynamic and static measures of brain connectivity. Our comparisons revealed similar relative trait ranking in prediction accuracies for the different edge conceptualizations. However, corresponding CAR scores revealed differential feature rankings, suggesting that the different edge definitions provide complementary information. For age, whereas previous studies have shown that dFC decreases with increased age (74, 75), we obtained noticeably poorer prediction accuracy for dFC than the other feature sets, implying that age is better characterized by static than dynamic FC.

Overall, our results suggest higher dFC within a frontal-DMN cluster in individuals with higher intelligence and educational attainment. However, interpretations of the dFC and bandpass filtered sFC results should be done with care, as they performed worse than the feature set with only sFC edges. One exception was that the feature set with all FC-types performed marginally better when predicting age and classifying sex compared to sFC alone, which may suggest that there is added predictive value when the signal is strong. A recent study found that the discriminative properties of FC vary across parcellation schemes and frequencies, with ICA-based parcellations revealing greater discriminability at high frequencies compared to other parcellations (76).

We were not able to predict dimensional measures of neuroticism, depression or anxiety, consistent with a smaller independent study (77) and a recent large-scale multi-site study (78). One explanation for the lack of brain FC associations, particularly with regards to depression is its diversity in symptom profiles (36), and phenomenological overlap with other clinical domains (79). Some studies have attempted to identify putative subgroups of patients

by using data-driven clustering based on symptoms (77, 80) or brain functional connectivity patterns (81, 82). In line with recent work questioning the robustness and generalizability of such clustering approaches (30), our current results do not support a simple link between fMRI-based brain connectivity and sub-clinical manifestations of depression and anxiety.

To the best of our knowledge, this is the first study that uses machine learning to predict polygenic scores based on resting-state brain FC measures. A recent study demonstrated significant prediction accuracy for polygenic scores for autism using grey matter volumes, but not for attention deficit-hyperactivity disorder, bipolar disorder or schizophrenia (83). However, the sample size was small compared to the current study. Large sample sizes are needed to establish reliable estimates for the neuronal correlates of measures with weak associations (34, 84). Relatedly, our findings illustrate that the correlation between raw and predicted scores may overestimate model performance, at least when model performance is low. Unlike R^2, MAE and RMSE, correlation coefficients are affected by scaling and location of the predicted scores relative to the raw scores, and, in contrast to MAE and RMSE, assumes linearity and homoscedasticity. Future studies using machine learning to predict continuous measures should carefully consider the choice of metric used for evaluating model performance (85), and reporting converging evidence of model fit and robustness may increase the reliability of the findings.

Despite the overall low predictive accuracy of the polygenic scores, we observed a relatively high positive correlation between the edge-wise feature importance of trait level educational attainment and intelligence with their respective polygenic scores, indicating some shared signal. Whereas the overall model performance was low, it is conceivable that any genetic pleiotropy between complex human traits and the brain is stronger for other imaging modalities. Indeed, some studies have demonstrated an association between cortical structure and polygenic scores for schizophrenia (86, 87), which are supported by a recent

large-scale UKB study reporting thinner fronto-temporal cortex with higher polygenic risk (54). However, the variance explained by polygenic scores, such as those for schizophrenia, for brain measures like gray matter volume, tend to be low (88).

The low prediction accuracy obtained for polygenic scores was observed both when applying a liberal and a more conservative initial p-value threshold when computing the polygenic score, and when deriving general polygenic scores using PCA across a range of thresholds. Hence, the low predictive accuracy cannot simply be explained by the number of independent SNPs feeding into the cumulative score. Relatedly, the poor accuracy may also be partly explained by the small amount of trait variance accounted for by the polygenic score. For example, in the most recent GWAS the trait variance explained for educational polygenic scores was 12% and polygenic scores for cognitive performance explained 7-10% of the trait variance (6). Further, based on case-control differences, the polygenic score for schizophrenia (8), MDD (9), and anxiety (89) explained at most 7%, 1.9%, 2.3% and 2.1% of variance, respectively. Although the small proportion of explained variance extends to somatic diseases such as coronary artery disease and breast cancer (90), the low predictive accuracy of the polygenic risk scores, which limits its current clinical utility (91), may partly be due to the heterogeneity of complex human traits and disorders, and may disguise true genetic pleiotropy between brain features and the polygenic architecture of complex traits. Dimensional approaches such as normative modeling (92–94) or brain age prediction (95) may reveal stronger shared signal. Many studies have shown that complex traits and disorders have substantial genetic overlap (96, 97) which may dilute the signal-to-noise ratio and specificity of polygenic scores. Future studies applying GWAS results with more power and novel techniques for boosting the shared genetic signal between traits (98, 99) may reveal stronger evidence of pleiotropy between brain FC and the polygenic architecture of complex traits. To more fully establish the clinical utility of polygenic scores, there is also a need to

evaluate treatment response rates of psychiatric disorders across scores (100). Taken together with other inherent limitations (see Supplements), the converging pattern across metrics of model performance indicate chance-level performance of brain FC for polygenic scores.

In conclusion, based on fMRI data from 10,343 individuals we have demonstrated high prediction accuracy of fMRI-based brain connectivity for age and sex, as well as moderate yet above chance level accuracy for educational attainment and intelligence, which are complex yet highly relevant characteristics and indicators of individual adaptation and brain and mental health. In contrast, we obtained chance-level prediction accuracy for dimensional measures of depression, anxiety and neuroticism, in addition to their genetic underpinnings based on the respective polygenic scores and polygenic risk for schizophrenia. These findings support the link between educational attainment and intellectual abilities and the organization of the brain functional connectome, and provide a reference for imaging studies mapping the functional brain mechanisms of clinical and genetic risk for mental disorders.

Acknowledgments and Disclosures

The authors were funded by the Research Council of Norway (213837, 223723, 229129, 204966, 249795), the South-Eastern Norway Regional Health Authority (2014097, 2015073, 2016083, 2017112), the European Research Council under the European Union's Horizon 2020 research and innovation program (ERC StG, Grant 802998), the Department of Psychology, University of Oslo and the KG Jebsen Stiftelsen. The permutation testing was performed using resources provided by UNINETT Sigma2 - the National Infrastructure for High Performance Computing and Data Storage in Norway. This research has been conducted using the UK Biobank Resource (access code 27412). This work has been posted on bioRxiv (https://www.biorxiv.org/content/10.1101/609586v1).

OA has previously received speakers honoraria from Lundbeck and Sunovion. NIL has previously received consultancy fees and travel expenses from Lundbeck. All other authors report no biomedical financial interests or potential conflicts of interest.

References

1. Walker ER, McGee RE, Druss BG (2015): Mortality in mental disorders and global disease burden implications. *JAMA Psychiatry*. 72: 334–341.
2. Insel TR (2015): Brain disorders? Precisely. *Science*. 348: 499–500.
3. Cuthbert BN, Insel TR (2012): Toward the future of psychiatric diagnosis: the seven pillars of RDoC. *Am J Psychiatry*. 11: 126.
4. Insel TR (2014): The NIMH Research Domain Criteria (RDoC) Project: Precision medicine for psychiatry. *Am J Psychiatry*. 171: 395–397.
5. Polderman TJC, Benyamin B, de Leeuw CA, Sullivan PF, van Bochoven A, Visscher PM, Posthuma D (2015): Meta-analysis of the heritability of human traits based on fifty years of twin studies. *Nat Genet*. 47: 702–709.
6. Lee JJ, Wedow R, Okbay A, Kong E, Maghzian O, Zacher M, *et al.* (2018): Gene discovery and polygenic prediction from a genome-wide association study of educational attainment in 1.1 million individuals. *Nat Genet*. 50: 1112–1121.
7. Savage JE, Jansen PR, Stringer S, Watanabe K, Bryois J, Leeuw CA de, *et al.* (2018): Genome-wide association meta-analysis in 269,867 individuals identifies new genetic and functional links to intelligence. *Nat Genet*. 50: 912–919.
8. Ripke S, Neale BM, Corvin A, Walters JT, Farh K-H, Holmans PA, *et al.* (2014): Biological insights from 108 schizophrenia-associated genetic loci. *Nature*. 511: 421–427.
9. Wray NR, Ripke S, Mattheisen M, Trzaskowski M, Byrne EM, Abdellaoui A, *et al.* (2018): Genome-wide association analyses identify 44 risk variants and refine the genetic architecture of major depression. *Nat Genet*. 50: 668–681.
10. Ikeda M, Takahashi A, Kamatani Y, Okahisa Y, Kunugi H, Mori N, *et al.* (2018): A genome-wide association study identifies two novel susceptibility loci and trans

population polygenicity associated with bipolar disorder. *Mol Psychiatry*. 23: 639–647.

11. Widiger TA, Oltmanns JR (2017): Neuroticism is a fundamental domain of personality with enormous public health implications. *World Psychiatry*. 16: 144–145.
12. Nagel M, Jansen PR, Stringer S, Watanabe K, de Leeuw CA, Bryois J, *et al.* (2018): Meta-analysis of genome-wide association studies for neuroticism in 449,484 individuals identifies novel genetic loci and pathways. *Nat Genet*. 50: 920–927.
13. Nagel M, Watanabe K, Stringer S, Posthuma D, Sluis S van der (2018): Item-level analyses reveal genetic heterogeneity in neuroticism. *Nat Commun*. 9: 905.
14. Luciano M, Hagenaars SP, Davies G, Hill WD, Clarke T-K, Shirali M, *et al.* (2018): Association analysis in over 329,000 individuals identifies 116 independent variants influencing neuroticism. *Nat Genet*. 50: 6–11.
15. Gale CR, Hagenaars SP, Davies G, Hill WD, Liewald DCM, Cullen B, *et al.* (2016): Pleiotropy between neuroticism and physical and mental health: findings from 108 038 men and women in UK Biobank. *Transl Psychiatry*. 6: e791.
16. Deary IJ, Penke L, Johnson W (2010): The neuroscience of human intelligence differences. *Nat Rev Neurosci*. 11: 201–211.
17. Strenze T (2007): Intelligence and socioeconomic success: A meta-analytic review of longitudinal research. *Intelligence*. 35: 401–426.
18. Posthuma D, De Geus EJC, Baaré WFC, Hulshoff Pol HE, Kahn RS, Boomsma DI (2002): The association between brain volume and intelligence is of genetic origin. *Nat Neurosci*. 5: 83–84.
19. Shen X, Cox SR, Adams MJ, Howard DM, Lawrie SM, Ritchie SJ, *et al.* (2018): Resting-state connectivity and its association with cognitive performance, educational

attainment, and household income in the UK Biobank. *Biol Psychiatry Cogn Neurosci Neuroimaging*. 3: 878–886.

20. Alnæs D, Kaufmann T, Doan NT, Córdova-Palomera A, Wang Y, Bettella F, *et al.* (2018): Association of heritable cognitive ability and psychopathology with white matter properties in children and adolescents. *JAMA Psychiatry*. 75: 287–295.
21. MacKenzie LE, Uher R, Pavlova B (2019): Cognitive performance in first-degree relatives of individuals with vs without major depressive disorder: A meta-analysis. *JAMA Psychiatry*. 76: 297–305.
22. Kendler KS, Ohlsson H, Keefe RSE, Sundquist K, Sundquist J (2018): The joint impact of cognitive performance in adolescence and familial cognitive aptitude on risk for major psychiatric disorders: A delineation of four potential pathways to illness. *Mol Psychiatry*. 23: 1076–1083.
23. Wraw C, Deary IJ, Gale CR, Der G (2015): Intelligence in youth and health at age 50. *Intelligence*. 53: 23–32.
24. Conti G, Heckman J, Urzua S (2010): The education-health gradient. *Am Econ Rev*. 100: 234–238.
25. Plomin R, Kovas Y (2005): Generalist genes and learning disabilities. *Psychol Bull*. 131: 592–617.
26. Elliott LT, Sharp K, Alfaro-Almagro F, Shi S, Miller KL, Douaud G, *et al.* (2018): Genome-wide association studies of brain imaging phenotypes in UK Biobank. *Nature*. 562: 210–216.
27. Mulders PC, van Eijndhoven PF, Schene AH, Beckmann CF, Tendolkar I (2015): Resting-state functional connectivity in major depressive disorder: A review. *Neurosci Biobehav Rev*. 56: 330–344.

28. Wojtalik JA, Smith MJ, Keshavan MS, Eack SM (2017): A systematic and meta-analytic review of neural correlates of functional outcome in schizophrenia. *Schizophr Bull*. 43: 1329–1347.

29. Mouchlianitis E, McCutcheon R, Howes OD (2016): Brain-imaging studies of treatment-resistant schizophrenia: a systematic review. *Lancet Psychiatry*. 3: 451–463.

30. Dinga R, Schmaal L, Penninx BWJH, van Tol MJ, Veltman DJ, van Velzen L, *et al.* (2019): Evaluating the evidence for biotypes of depression: Methodological replication and extension of Drysdale et al. (2017). *NeuroImage Clin*. 101796.

31. Paulus MP, Thompson WK (2019): The challenges and opportunities of small effects: The new normal in academic psychiatry. *JAMA Psychiatry*. 76: 353–354.

32. Kapur S, Phillips AG, Insel TR (2012): Why has it taken so long for biological psychiatry to develop clinical tests and what to do about it? *Mol Psychiatry*. 17: 1174–1179.

33. Button KS, Ioannidis JP, Morkrysz C, Nosek BA, Flint J, Robinson ESJ, Munafò MR (2013): Power failure: why small sample size undermines the reliability of neuroscience. - PubMed - NCBI. *Nat Rev Neurosci*. 14: 365–376.

34. Westlye LT, Alnæs D, Meer D van der, Kaufmann T, Andreassen OA (2019): Population-based mapping of polygenic risk for schizophrenia on the human brain: New opportunities to capture the dimensional aspects of severe mental disorders. *Biol Psychiatry*. 86: 499–501.

35. Gong Q, He Y (2015): Depression, neuroimaging and connectomics: a selective overview. *Biol Psychiatry*. 77: 223–235.

36. Fried EI, Nesse RM (2015): Depression is not a consistent syndrome: An investigation of unique symptom patterns in the STAR*D study. *J Affect Disord*. 172: 96–102.

37. Liang SG, Greenwood TA (2015): The impact of clinical heterogeneity in schizophrenia on genomic analyses. *Schizophr Res*. 161: 490–495.

38. Marquand AF, Wolfers T, Mennes M, Buitelaar J, Beckmann CF (2016): Beyond lumping and splitting: A review of computational approaches for stratifying psychiatric disorders. *Biol Psychiatry Cogn Neurosci Neuroimaging*. 1: 433–447.

39. Adhikari BM, Jahanshad N, Shukla D, Glahn DC, Blangero J, Reynolds RC, *et al.* (2018): Heritability estimates on resting state fMRI data using ENIGMA analysis pipeline. *Pac Symp Biocomput Pac Symp Biocomput*. 23: 307–318.

40. Glahn DC, Winkler AM, Kochunov P, Almasy L, Duggirala R, Carless MA, *et al.* (2010): Genetic control over the resting brain. *Proc Natl Acad Sci U S A*. 107: 1223–1228.

41. Thompson WH, Fransson P (2015): The frequency dimension of fMRI dynamic connectivity: Network connectivity, functional hubs and integration in the resting brain. *NeuroImage*. 121: 227–242.

42. Buzsáki G, Draguhn A (2004): Neuronal oscillations in cortical networks. *Science*. 304: 1926–1929.

43. Knyazev GG (2007): Motivation, emotion, and their inhibitory control mirrored in brain oscillations. *Neurosci Biobehav Rev*. 31: 377–395.

44. Smith SM, Nichols TE, Vidaurre D, Winkler AM, Behrens TEJ, Glasser MF, *et al.* (2015): A positive-negative mode of population covariation links brain connectivity, demographics and behavior. *Nat Neurosci*. 18: 1565–1567.

45. Sudlow C, Gallacher J, Allen N, Beral V, Burton P, Danesh J, *et al.* (2015): UK biobank: an open access resource for identifying the causes of a wide range of complex diseases of middle and old age. *PLoS Med*. 12: e1001779.

46. Miller KL, Alfaro-Almagro F, Bangerter NK, Thomas DL, Yacoub E, Xu J, *et al.* (2016): Multimodal population brain imaging in the UK Biobank prospective epidemiological study. *Nat Neurosci*. 19: 1523–1536.

47. Alfaro-Almagro F, Jenkinson M, Bangerter NK, Andersson JLR, Griffanti L, Douaud G, *et al.* (2018): Image processing and quality control for the first 10,000 brain imaging datasets from UK Biobank. *NeuroImage*. 166: 400–424.

48. Okbay A, Beauchamp JP, Fontana MA, Lee JJ, Pers TH, Rietveld CA, *et al.* (2016): Genome-wide association study identifies 74 loci associated with educational attainment. *Nature*. 533: 539–542.

49. Hagenaars SP, Harris SE, Davies G, Hill WD, Liewald DCM, Ritchie SJ, *et al.* (2016): Shared genetic aetiology between cognitive functions and physical and mental health in UK Biobank (N=112 151) and 24 GWAS consortia. *Mol Psychiatry*. 21: 1624–1632.

50. Euesden J, Lewis CM, O'Reilly PF (2015): PRSice: Polygenic Risk Score software. *Bioinforma Oxf Engl*. 31: 1466–1468.

51. Howard DM, Adams MJ, Shirali M, Clarke T-K, Marioni RE, Davies G, *et al.* (2018): Genome-wide association study of depression phenotypes in UK Biobank identifies variants in excitatory synaptic pathways. *Nat Commun*. 9: 1470.

52. Otowa T, Hek K, Lee M, Byrne EM, Mirza SS, Nivard MG, *et al.* (2016): Meta-analysis of genome-wide association studies of anxiety disorders. *Mol Psychiatry*. 21: 1391–1399.

53. Ruderfer DM, Fanous AH, Ripke S, McQuillin A, Amdur RL, Schizophrenia Working Group of the Psychiatric Genomics Consortium, *et al.* (2014): Polygenic dissection of diagnosis and clinical dimensions of bipolar disorder and schizophrenia. *Mol Psychiatry*. 19: 1017–1024.

54. Alnæs D, Kaufmann T, Meer D van der, Córdova-Palomera A, Rokicki J, Moberget T, *et al.* (2019): Brain heterogeneity in schizophrenia and its association with polygenic risk. *JAMA Psychiatry*. doi: 10.1001/jamapsychiatry.2019.0257.

55. Smith SM, Miller KL, Salimi-Khorshidi G, Webster M, Beckmann CF, Nichols TE, *et al.* (2011): Network modelling methods for FMRI. *NeuroImage*. 54: 875–891.

56. Friedman J, Hastie T, Tibshirani R (2008): Sparse inverse covariance estimation with the graphical lasso. *Biostat Oxf Engl*. 9: 432–441.

57. Kaufmann T, Skåtun KC, Alnæs D, Doan NT, Duff EP, Tønnesen S, *et al.* (2015): Disintegration of sensorimotor brain networks in schizophrenia. *Schizophr Bull*. 41: 1326–1335.

58. Ledoit O, Wolf M (2003): Improved estimation of the covariance matrix of stock returns with an application to portfolio selection. *J Empir Finance*. 10: 603–621.

59. Glerean E, Salmi J, Lahnakoski JM, Jääskeläinen IP, Sams M (2012): Functional magnetic resonance imaging phase synchronization as a measure of dynamic functional connectivity. *Brain Connect*. 2: 91–101.

60. Córdova-Palomera A, Kaufmann T, Persson K, Alnæs D, Doan NT, Moberget T, *et al.* (2017): Disrupted global metastability and static and dynamic brain connectivity across individuals in the Alzheimer's disease continuum. *Sci Rep*. 7:40268. doi: 10.1038/srep40268.

61. Deco G, Kringelbach ML (2016): Metastability and coherence: Extending the communication through coherence hypothesis using a whole-brain computational perspective. *Trends Neurosci*. 39: 125–135.

62. R Core Team (2017): *R: A language and environment for statistical computing. R Foundation for Statistical Computing*. Vienna, Austria: R Foundation for Statistical Computing. Retrieved from https://www.R-project.org/.

63. Schäfer J, Strimmer K (2005): A shrinkage approach to large-scale covariance matrix estimation and implications for functional genomics. *Stat Appl Genet Mol Biol*. 4: Article32.

64. Zuber V, Strimmer K (2011): High-dimensional regression and variable selection using CAR Scores. *Stat Appl Genet Mol Biol*. 10. doi: 10.2202/1544-6115.1730.

65. Kessy A, Lewin A, Strimmer K (2018): Optimal whitening and decorrelation. *Am Stat*. 72: 309–314.

66. Finn ES, Shen X, Scheinost D, Rosenberg MD, Huang J, Chun MM, *et al.* (2015): Functional connectome fingerprinting: identifying individuals using patterns of brain connectivity. *Nat Neurosci*. 18: 1664–1671.

67. Ferguson MA, Anderson JS, Spreng RN (2017): Fluid and flexible minds: Intelligence reflects synchrony in the brain's intrinsic network architecture. *Netw Neurosci Camb Mass*. 1: 192–207.

68. Dubois J, Galdi P, Paul LK, Adolphs R (2018): A distributed brain network predicts general intelligence from resting-state human neuroimaging data. *Philos Trans R Soc Lond B Biol Sci*. 373. doi: 10.1098/rstb.2017.0284.

69. Jiang R, Calhoun VD, Fan L, Zuo N, Jung R, Qi S, *et al.* (2019): Gender differences in connectome-based predictions of individualized intelligence quotient and sub-domain scores. *Cereb Cortex N Y N 1991*. doi: 10.1093/cercor/bhz134.

70. Andrews-Hanna JR, Snyder AZ, Vincent JL, Lustig C, Head D, Raichle ME, Buckner RL (2007): Disruption of large-scale brain systems in advanced aging. *Neuron*. 56: 924–935.

71. Damoiseaux JS, Beckmann CF, Arigita EJS, Barkhof F, Scheltens P, Stam CJ, *et al.* (2008): Reduced resting-state brain activity in the "default network" in normal aging. *Cereb Cortex N Y N 1991*. 18: 1856–1864.

72. Grady CL, Protzner AB, Kovacevic N, Strother SC, Afshin-Pour B, Wojtowicz M, *et al.* (2010): A multivariate analysis of age-related differences in default mode and task-

positive networks across multiple cognitive domains. *Cereb Cortex N Y N 1991*. 20: 1432–1447.

73. He T, Kong R, Holmes A, Nguyen M, Sabuncu M, Eickhoff SB, *et al.* (2018): Do deep neural networks outperform kernel regression for functional connectivity prediction of behavior? *bioRxiv*. 473603.

74. Viviano RP, Raz N, Yuan P, Damoiseaux JS (2017): Associations between dynamic functional connectivity and age, metabolic risk, and cognitive performance. *Neurobiol Aging*. 59: 135–143.

75. Chen Y, Zhao X, Zhang X, Liu Y, Zhou P, Ni H, *et al.* (2018): Age-related early/late variations of functional connectivity across the human lifespan. *Neuroradiology*. 60: 403–412.

76. Sala-Llonch R, Smith SM, Woolrich M, Duff EP (2019): Spatial parcellations, spectral filtering, and connectivity measures in fMRI: Optimizing for discrimination. *Hum Brain Mapp*. 40: 407–419.

77. Maglanoc LA, Landrø NI, Jonassen R, Kaufmann T, Córdova-Palomera A, Hilland E, Westlye LT (2019): Data-driven clustering reveals a link between symptoms and functional brain connectivity in depression. *Biol Psychiatry Cogn Neurosci Neuroimaging*. 4: 16–26.

78. Yan C-G, Chen X, Li L, Castellanos FX, Bai T-J, Bo Q-J, *et al.* (2019): Reduced default mode network functional connectivity in patients with recurrent major depressive disorder. *Proc Natl Acad Sci*. 201900390.

79. Lamers F, van Oppen P, Comijs HC, Smit JH, Spinhoven P, van Balkom AJLM, *et al.* (2011): Comorbidity patterns of anxiety and depressive disorders in a large cohort study: the Netherlands Study of Depression and Anxiety (NESDA). *J Clin Psychiatry*. 72: 341–348.

80. Lamers F, de Jonge P, Nolen WA, Smit JH, Zitman FG, Beekman ATF, Penninx BWJH (2010): Identifying depressive subtypes in a large cohort study: results from the Netherlands Study of Depression and Anxiety (NESDA). *J Clin Psychiatry*. 71: 1582–1589.

81. Drysdale AT, Grosenick L, Downar J, Dunlop K, Mansouri F, Meng Y, *et al.* (2017): Resting-state connectivity biomarkers define neurophysiological subtypes of depression. *Nat Med*. 23: 28–38.

82. Price RB, Gates K, Kraynak TE, Thase ME, Siegle GJ (2017): Data-driven subgroups in depression derived from directed functional connectivity paths at rest. *Neuropsychopharmacology*. 42: 2623–2632.

83. Ranlund S, Rosa MJ, de Jong S, Cole JH, Kyriakopoulos M, Fu CHY, *et al.* (2018): Associations between polygenic risk scores for four psychiatric illnesses and brain structure using multivariate pattern recognition. *NeuroImage Clin*. 20: 1026–1036.

84. Wolfers T, Buitelaar JK, Beckmann CF, Franke B, Marquand AF (2015): From estimating activation locality to predicting disorder: A review of pattern recognition for neuroimaging-based psychiatric diagnostics. *Neurosci Biobehav Rev*. 57: 328–349.

85. Dinga R, Penninx BWJH, Veltman DJ, Schmaal L, Marquand AF (2019): Beyond accuracy: Measures for assessing machine learning models, pitfalls and guidelines. *bioRxiv*. 743138.

86. Neilson E, Bois C, Gibson J, Duff B, Watson A, Roberts N, *et al.* (2017): Effects of environmental risks and polygenic loading for schizophrenia on cortical thickness. *Schizophr Res*. 184: 128–136.

87. Liu B, Zhang X, Cui Y, Qin W, Tao Y, Li J, *et al.* (2017): Polygenic risk for schizophrenia influences cortical gyrification in 2 independent general populations. *Schizophr Bull*. 43: 673–680.

88. Reus LM, Shen X, Gibson J, Wigmore E, Ligthart L, Adams MJ, *et al.* (2017): Association of polygenic risk for major psychiatric illness with subcortical volumes and white matter integrity in UK Biobank. *Sci Rep*. 7: 42140.

89. Demirkan A, Penninx BWJH, Hek K, Wray NR, Amin N, Aulchenko YS, *et al.* (2011): Genetic risk profiles for depression and anxiety in adult and elderly cohorts. *Mol Psychiatry*. 16: 773–783.

90. Khera AV, Chaffin M, Aragam KG, Haas ME, Roselli C, Choi SH, *et al.* (2018): Genome-wide polygenic scores for common diseases identify individuals with risk equivalent to monogenic mutations. *Nat Genet*. 50: 1219–1224.

91. Martin AR, Daly MJ, Robinson EB, Hyman SE, Neale BM (2019): Predicting polygenic risk of psychiatric disorders. *Biol Psychiatry*. 86: 97–109.

92. Wolfers T, Doan NT, Kaufmann T, Alnæs D, Moberget T, Agartz I, *et al.* (2018): Mapping the heterogeneous phenotype of schizophrenia and bipolar disorder using normative models. *JAMA Psychiatry*. 75: 1146–1155.

93. Marquand AF, Rezek I, Buitelaar J, Beckmann CF (2016): Understanding heterogeneity in clinical cohorts using normative models: Beyond case-control studies. *Biol Psychiatry*. 80: 552–561.

94. Marquand AF, Kia SM, Zabihi M, Wolfers T, Buitelaar JK, Beckmann CF (2019): Conceptualizing mental disorders as deviations from normative functioning. *Mol Psychiatry*. 1.

95. Kaufmann T, van der Meer D, Doan NT, Schwarz E, Lund MJ, Agartz I, *et al.* (2019): Common brain disorders are associated with heritable patterns of apparent aging of the brain. *Nat Neurosci*. 22: 1617–1623.

96. Smeland OB, Bahrami S, Frei O, Shadrin A, O'Connell K, Savage J, *et al.* (2019): Genome-wide analysis reveals extensive genetic overlap between schizophrenia, bipolar disorder, and intelligence. *Mol Psychiatry*. doi: 10.1038/s41380-018-0332-x.

97. Witt SH, Streit F, Jungkunz M, Frank J, Awasthi S, Reinbold CS, *et al.* (2017): Genome-wide association study of borderline personality disorder reveals genetic overlap with bipolar disorder, major depression and schizophrenia. *Transl Psychiatry*. 7: e1155.

98. Andreassen OA, Thompson WK, Schork AJ, Ripke S, Mattingsdal M, Kelsoe JR, *et al.* (2013): Improved detection of common variants associated with schizophrenia and bipolar disorder using pleiotropy-informed conditional false discovery rate. *PLoS Genet*. 9: e1003455.

99. Frei O, Holland D, Smeland OB, Shadrin AA, Fan CC, Maeland S, *et al.* (2019): Bivariate causal mixture model quantifies polygenic overlap between complex traits beyond genetic correlation. *Nat Commun*. 10: 2417.

100. Gibson G (2019): On the utilization of polygenic risk scores for therapeutic targeting. *PLoS Genet*. 15: e1008060.